VOL 42 NO. 4 | July 2011

Journal of the Taiwan Institute of Chemical Engineers

台灣化學工程學會會誌

Published by the Taiwan Institute of
Chemical Engineers,
Taipei, Taiwan, Republic of China

ELSEVIER

ISSN 1876-1070
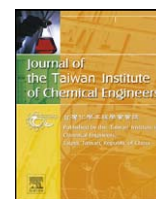
Drug design for mPGES-1 from traditional Chinese medicine database: A screening, docking, QSAR, molecular dynamics, and pharmacophore mapping study

Tung-Ti Chang [a,b], Mao-Feng Sun [a,c], Yung-Hao Wong [a], Shun-Chieh Yang [a], Kuan-Chung Chen [a], Hsin-Yi Chen [d], Fuu-Jen Tsai [d,e], Calvin Yu-Chian Chen [a,d,f,*]

[a] Laboratory of Computational and Systems Biology, School of Chinese Medicine, China Medical University, Taichung 40402, Taiwan
[b] Department of Chinese Pediatrics, China Medical University Hospital, Taiwan
[c] Department of Acupuncture, China Medical University Hospital, Taiwan
[d] Department of Bioinformatics, Asia University, Taichung 41354, Taiwan
[e] Department of Medical Genetics, Pediatrics and Medical Research, China Medical University Hospital and College of Chinese Medicine, China Medical University, Taichung 40402, Taiwan
[f] Computational and Systems Biology, Massachusetts Institute of Technology, Cambridge, MA 02139, USA

ABSTRACT

To search for new anti-inflammatory that can replace the current COX-1 and COX-2 inhibitors, virtual screening by molecular docking of traditional Chinese medicine (TCM) molecules into microsomal prostaglandin E$_2$ synthase (mPGES-1) glutathione binding site was performed. To compare the top ranking derivatives with other mPGES-1 inhibitors, we constructed QSAR models using comparative molecular force field analysis (CoMFA) and comparative molecular similarity indices analysis (CoMSIA). The CoMFA model had a non-cross-validated coefficient (r^2) and a cross-validated coefficient (q^2) of 0.960 and 0.597. The r^2 and q^2 for CoMSIA (S + H + D) was 0.931 and 0.719, respectively. The top three TCM derivatives all can map into the respective steric, hydrophobic and hydrogen bond donor force fields. The top ranking TCM molecules were taken for *de novo* design; the top three *de novo* products were further analyzed using molecular dynamics simulation and qualitative structure–activity relationship (QSAR) model. Derivative, 2-O-caffeoyl tartaric acid-Evo_2, glucogallin-Evo_1 and 4-O-feruloylquinic acid-Evo_7, all had conserved hydrogen bond networks to key residues Arg38 and Arg70 during the 20 ns molecular dynamics simulation. In addition, all derivative–protein complexes had total energy lower the control–protein complex. Combining the results from molecular dynamics simulation and CoMFA/CoMSIA, we suggest 2-O-caffeoyl tartaric acid-Evo_2, glucogallin-Evo_1 and 4-O-feruloylquinic acid-Evo_7 as potent mPGES-1 inhibitors.

© 2010 Taiwan Institute of Chemical Engineers. Published by Elsevier B.V. All rights reserved.

1. Introduction

Prostaglandins, products of prostanoids synthesis, are autocrines that are produced in various parts of human body. Prostaglandin E$_2$ (PGE$_2$), the most abundant subtype of prostaglandins, is the product from the action of prostaglandin E synthases on prostaglandin H$_2$ (Hara et al., 2010). To date, there are three known classes of prostaglandin E synthases, namely cytosolic PGE synthase (cPGES) and two membrane-bound synthases, mPGES-1 and mPGES-2 (Hara et al., 2010). The mPGES-1 protein, unlike the other PGE synthases, is not constitutively expressed and can be induced in response to inflammatory stimuli.

In the past, non-steroidal anti-inflammatory drugs (NSAIDs) have been designed to target COX-1 and COX-1, the upstream enzyme for producing prostaglandin H$_2$. However, long-term suppression of prostanoid biosynthesis by using COX-1 and COX-2 inhibitors can have severe side effects, including gastrointestinal injury and renal irritation (Koeberle and Werz, 2009). Current evidences suggest that suppression of mPGES-1 activity can be considered as an alternative anti-inflammatory approach. Since mPGES-1 is functionally coupled to COX-2 and is also being responsible for excessive PGE$_2$, its inhibitions are, therefore, related to inflammation, pain, fever, atherosclerosis and tumorigenesis.

* Corresponding author at: Laboratory of Computational and Systems Biology, School of Chinese Medicine, China Medical University, Taichung 40402, Taiwan. Tel.: +886 4 22053366x3326/+1 617 353 7123.
E-mail addresses: ycc@mail.cmu.edu.tw, ycc929@MIT.EDU (C.-C. Chen).

To develop novel anti-inflammatory agents, TCM Database@-Taiwan (http://tcm.cmu.edu.tw), the current world largest small molecule database on traditional Chinese medicine, was employed in docking. Natural compounds isolated from TCM are gaining attention in the last few, and studies have been done already on compounds, such as emodin or gallic acid and many more, to investigate their potential effects to cellular process (Chen, 2009d; Chen et al., 2010b; Lin et al., 2010; Liu et al., 2010; Lo et al., 2010). In addition to screening of TCM database, we used both structure-based and ligand-based approaches to further validate and support the bioactivity of the lead candidates. Both strategies have been implemented in drug researches in the past, and we have successfully used both techniques in designing anti-viral, anti-inflammatory, and anti-tumor agents (Chang et al., 2010; Chen, 2008, 2009a,b,c,e,f, 2010a,b; Chen and Chen, 2007, 2010; Chen et al., 2009a,b, 2010a; Huang et al., 2010a,b,c).

2. Materials and methods

2.1. Docking

A total of 20,000 traditional Chinese medicine compounds were downloaded from TCM Database@Taiwan (http://tcm.cmu.edu.tw) and docked into the glutathione binding site of mPGES-1. All the ligands were pre-treated with force field of CHARMm, and all the missing hydrogen were added. The protein model used for docking was downloaded from Protein Data Bank (PDB: 3DWW (Jegerschold et al., 2008)). The nature substrate for mPGES-1, glutathione (γ-L-glutamyl-L-cysteinyl-glycine), which co-crystallized with mPGES-1 by electron crystallography, was used as the control molecule. The binding location of glutathione found in the protein crystal was set as the docking site.

Table 1

TCM docking results. Only the top 10 candidates and controls are shown.

Compound	DS	-PMF04	Jain	Ludi1	Ludi2	Ludi 3
2-O-caffeoyl tartaric acid	215.079	144.63	5.42	870	698	789
Chicoric acid	206.092	177.22	5.00	915	694	826
Mumefural	201.985	136.75	8.50	1028	822	799
2-O-feruloyl tartaric acid	198.739	145.13	5.16	833	661	693
Rosmarinic acid	148.434	145.59	5.40	971	743	921
Quinic acid	143.961	106.56	1.49	557	487	475
Genipinic acid	142.772	110.31	2.53	530	467	651
Digallic acid	142.547	147.27	1.67	953	708	848
5-O-feruloylquinic acid	142.462	149.26	6.90	1011	784	865
4-O-feruloylquinic acid	140.488	142.14	7.45	946	746	878
Glutathione	66.787	127.28	6.39	564	447	412

DS: Dock Score; PMF: Potential of Mean Force.

Table 2

Docking results for *de novo* products. The top 5 candidates are shown.

Compound	DS	-PMF04	Jain	Ludi1	Ludi2	Ludi3
2-O-caffeoyl tartaric acid-Evo_2	222.198	136.13	5.65	701	569	656
Glucogallin-Evo_1 1	169.762	158.84	6.12	1062	795	974
4-O-feruloylquinic acid-Evo_7	167.056	152.93	8.01	999	783	919
1-Caffeoylquinic acid-Evo_3	165.916	150.93	5.90	774	591	674
4-O-feruloylquinic acid-Evo_5	159.929	160.19	7.34	1071	822	950
Glutathione	66.787	127.28	6.39	564	447	412

DS: Dock Score; PMF: Potential of Mean Force.

Table 3

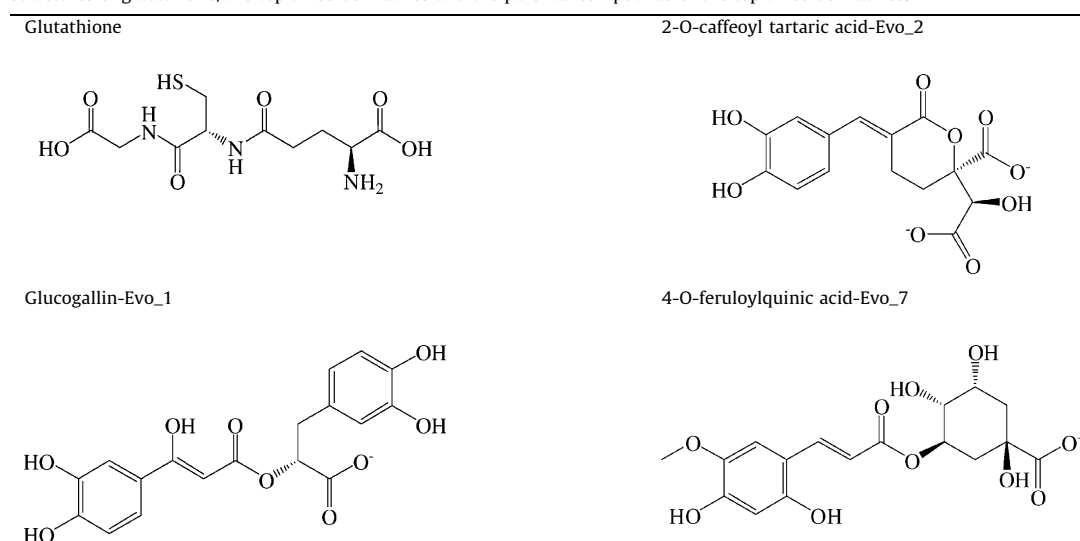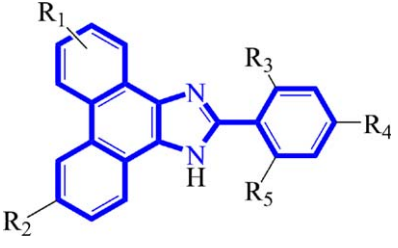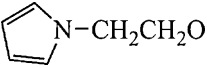Structures of glutathione, the top three derivatives and the parental compounds of the top three derivatives.
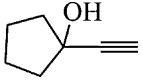
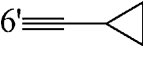| Glutathione	2-O-caffeoyl tartaric acid-Evo_2

Glucogallin-Evo_1	4-O-feruloylquinic acid-Evo_7
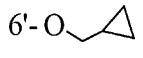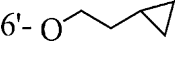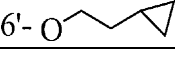
Table 4
The structure of the training set and the test set.

Index	R1	R_2	R_3	R_4	R_5
1	6'-Cl	Cl	NC	H	NC
2	H	H	Cl	H	F
3	6'-Cl	H	Cl	H	F
4	5'-Cl	H	Cl	H	F
5	6'-Br	H	Cl	H	F
6[a]	4'-Br	H	Cl	H	F
7	5'-Br	H	Cl	H	F
8	7'-Br	H	Cl	H	F
9	6'-Br	Br	Cl	H	F
10[a]	6'-Br	iPr	Cl	H	F
11	6'-Br	OMe	Cl	H	F
12	6'-Br	COMe	Cl	H	F
13	6'-Br	$HO(CF_3)_2C$	Cl	H	F
14[a]	6'-Br	$HO(CH_3)_2C$	Cl	H	F
15	6'-Me	Me	Cl	H	F
16	6'-COMe	COMe	Cl	H	F
17	$6'-C(CH_3)_2OH$	$HO(CF_3)_2C$	Cl	H	F
18	6'-Cl	$HO(CH_3)_2C$	NC	H	NC
19	6'-Cl	$MeSO_2$	NC	H	NC
20	6'-Cl	$NCCH_2CH_2CH_2O$	NC	H	NC
21[a]	6'-Cl		NC	H	NC

Index	R1	R_2	R_3	R_4	R_5
22	6'-Cl	$p-MeSO_2C_6H_4$	NC	H	NC
23	6'-Cl	$MeOCH_2C\equiv C$	NC	H	NC
24	6'-Cl	$3-PyridylC\equiv C$	NC	H	NC
25	6'-Cl	$4-PyridylC\equiv C$	NC	H	NC
26	6'-Cl		NC	H	NC

Index	R1	R_2	R_3	R_4	R_5
27[a]			NC	H	NC
28	6'-Et	$HO(CH_3)_2CC\equiv C$	NC	H	NC
29		$HO(CH_3)_2CC\equiv C$	NC	H	NC

Index	R1	R_2	R_3	R_4	R_5
30	6'-Cl	$HO(CH_3)_2CCH_2CH_2$	NC	H	NC
31[a]	6'-Cl	$HO(CH_3)_2CCH_2$	NC	H	NC
32		$HO(CH_3)_2CCH_2$	NC	H	NC

Index	R1	R_2	R_3	R_4	R_5
33	6'-OCH2CH2CH2CF3	$HO(CH_3)_2CCH_2$	NC	H	NC
34	$6'-OCH_2CH_2CH(CH3)2$	$HO(CH_3)_2CCH_2$	NC	H	NC
35	$6'-OCH_2CH(CH_3)_2$	$HO(CH_3)_2CCH_2$	NC	H	NC
36		$HO(CH_3)_2CCH_2$	NC	H	NC

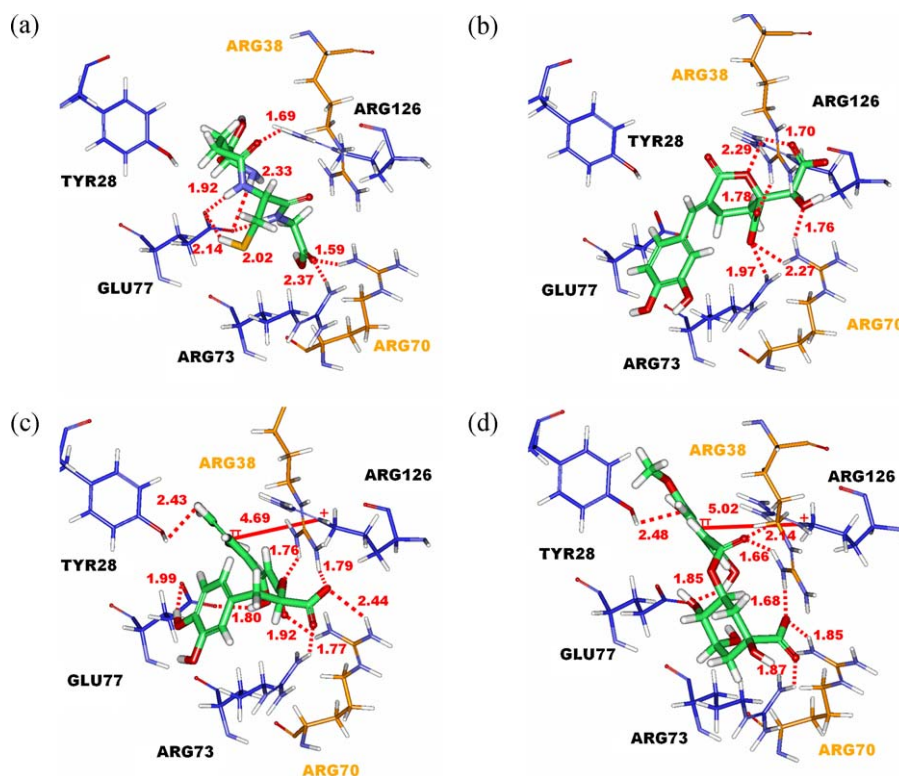| Index	R1	R_2	R_3	R_4	R_5
37		$HO(CH_3)_2CCH_2$	NC	F	NC

[a] Test set compounds.

Fig. 1. Docking poses of (a) glutathione, (b) 2-O-caffeoyl tartaric acid-Evo_2, (c) glucogallin-Evo_1, and (d) 4-O-feruloylquinic acid-Evo_7 in mPGES-1 glutathione binding site.

The LigandFit program (Venkatachalam et al., 2003) within Discovery Studio 2.5 was used to dock the TCM ingredients. LigandFit is a receptor-rigid docking algorithm that utilizes Monte Carlo simulation for generating ligand poses and a shape-matching filter for comparing ligand poses with binding site shape. Candidate ligand poses are then positioned into the binding site and followed by rigid body energy minimization.

Dock Score (Venkatachalam et al., 2003), Potential of Mean Force (PMF04) (Muegge and Martin, 1999), Jain (Jain, 1996) and Ludi (Bohm, 1998) were calculated for predicting receptor–ligand binding affinities. Dock Score was used as the primary scoring function for ranking the poses of each ligand and for selecting the poses. This scoring function is expressed as the sum of ligand internal energy and receptor–ligand interaction energy. The other scores, PMF04, Jain and Ludi, were calculated mainly for references. PMF04 calculates pairwise interactions of all inter-atomic pairs of a receptor–ligand system whereas Jain is based on lipophilic interactions, polar attractive and repulsive interactions, ligand entropy and solvation state of the protein and ligand. Ludi, on the other hand, is the sum of contribution from ideal hydrogen bond, ionic interaction, lipophilic interaction, and loss of internal degrees of freedom, translational entropy and rotational entropy of the ligand.

2.2. De novo design and Lipinski's Rule of Five

The top ranking TCM compounds from docking were input into De Novo Evolution protocol of Discovery Studio 2.5 for generating derivatives. This protocol based on LUDI (Bohm, 1992), which determines interaction sites suitable for hydrogen bond or hydrophobic interaction, fits Ludi fragments best complementing interaction sites and connects fitted fragments to a single molecule.

Table 5
Statistical data for CoMFA and CoMSIA.

	CoMFA	CoMSIA	Cross-validation		Non-cross-validation		
			ONC	q_{cv}^2	r^2	SEE	F
ONC	6	S	6	0.446	0.792	0.306	15.238
q_{cv}^2	0.597	H	6	0.733	0.956	0.141	86.480
SEE	0.135	D	6	0.167	0.432	0.506	3.043
r^2	0.960	A	6	0.420	0.786	0.311	14.711
F	95.361	S+H	5	0.724	0.948	0.151	90.623
		S+D	5	0.291	0.662	0.383	9.775
		S+A	5	0.459	0.807	0.289	20.896
		H+D	4	0.722	0.905	0.199	61.949
		H+A	6	0.480	0.924	0.185	48.584
		D+A	6	0.442	0.846	0.263	22.053
		S+H+D		0.719	0.931	0.176	54.319
		S+H+A	5	0.642	0.915	0.192	54.043
		S+D+A	5	0.501	0.836	0.267	25.455
		H+D+A	5	0.654	0.930	0.175	65.965
		S+H+D+A	6	0.630	0.940	0.164	62.960

ONC: optimal number of components; SEE: standard error of estimate; F: F-test value; PLS: partial least squares; S: steric; H: hydrophobic; D: hydrogen bond donor; A: hydrogen bond acceptor.
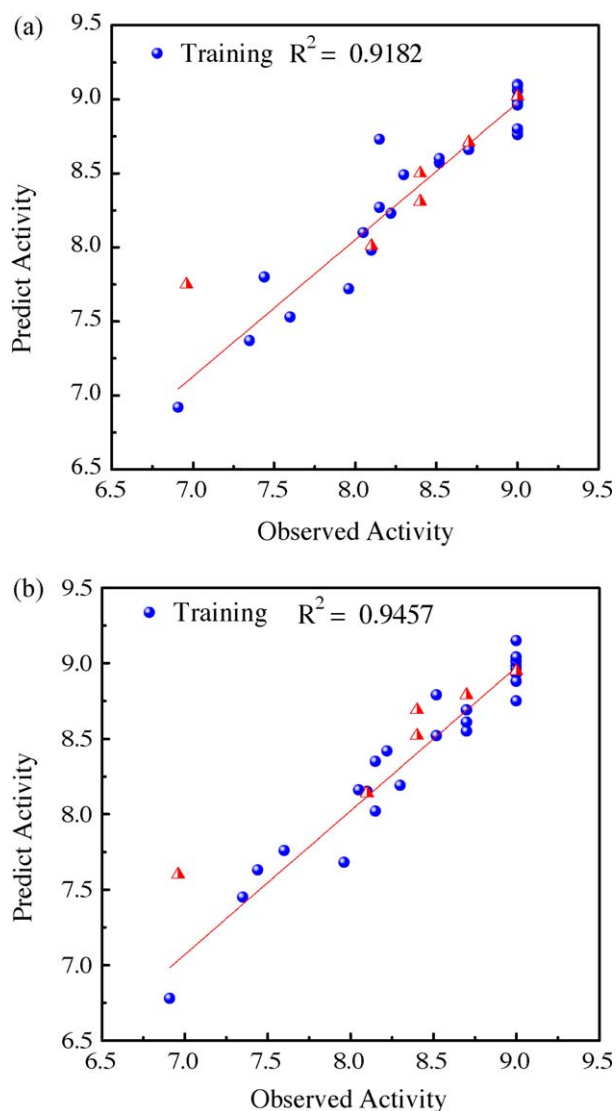
Fig. 2. Predicted pIC_{50} vs. experiment pIC_{50} for (a) CoMFA and (b) CoMSIA.

The evolution mode for generating derivatives was set to full evolution that builds molecules in an evolutionary fashion. The maximum number of generations, survivors and population size were set to 2, 3 and 10, respectively. Ludi scoring function (Ludi 3) was used to evaluate the fitness of the newly generated derivatives.

The generated derivatives, before re-docked back to protein to evaluate protein–ligand interactions, were screened with the Lipinski's Rule of Five (Lipinski et al., 2001). The derivatives that exceed the number of hydrogen bond donor and acceptors, the upper molecular weight limit, and the octanol–water coefficient were excluded from further analysis. An ADMET analysis was also performed to rule out derivatives that poses potential toxicity to human body. This is done in Discovery Studio 2.5.

2.3. CoMFA and CoMSIA

The structures of 37 phenanthrene imidazole based compounds used in this study were compiled from Giroux et al. (2009). The inhibitory potencies of these phenanthrene imidazoles were assessed in vitro using recombinant human mPGES-1 enzyme, and the reported IC_{50} values were means of at least two experiments (Mancini et al., 2001). The compounds were further divided into a training set of 31 compounds and a test set of 6 compounds. The selection for training set and test set was totally

Table 6
Predicted activity of the training set and the test set.

Compound	pIC_{50}	CoMFA		CoMSIA	
		Predicted	Residual	Predicted	Residual
1	9.00	8.79	0.21	8.75	0.25
2	7.44	7.80	−0.36	7.63	−0.19
3	8.30	8.49	−0.19	8.19	0.11
4	7.96	7.72	0.24	7.68	0.29
5	8.70	8.69	0.01	8.55	0.15
6[a]	6.96	7.75	−0.79	7.60	−0.64
7	7.60	7.53	0.07	7.76	−0.16
8	8.10	7.98	0.12	8.15	−0.05
9	8.52	8.57	−0.04	8.79	−0.27
10[a]	8.40	8.31	0.09	8.69	−0.29
11	8.22	8.23	−0.01	8.42	−0.20
14[a]	8.10	8.01	0.09	8.14	−0.04
15	9.00	8.76	0.24	8.93	0.07
17	8.15	8.73	−0.58	8.35	−0.20
18	8.15	8.27	−0.12	8.02	0.14
19	6.91	6.92	−0.01	6.78	0.13
20	7.35	7.37	−0.02	7.45	−0.10
21[a]	8.40	8.50	−0.10	8.52	−0.12
22	8.05	8.10	−0.05	8.16	−0.11
24	9.00	8.99	0.01	8.98	0.02
25	9.00	8.80	0.21	8.88	0.12
26	8.70	8.69	0.01	8.61	0.09
27[a]	8.70	8.71	−0.01	8.79	−0.09
28	9.00	8.97	0.03	8.96	0.04
30	9.00	9.10	−0.10	8.94	0.06
31[a]	9.00	9.02	−0.02	8.95	0.05
32	9.00	9.01	−0.01	9.15	−0.15
33	9.00	9.06	−0.06	9.02	−0.02
34	9.00	9.09	−0.09	9.01	−0.01
35	9.00	8.96	0.04	9.04	−0.04
36	8.70	8.66	0.04	8.69	0.01
37	8.52	8.60	−0.08	8.52	0.00

[a] Test set compounds.

random. Alignment of the training set molecules was performed using atom-fit module of SYBYL 8.0.

To build QSAR model using comparative force field analysis (CoMFA), the steric and electrostatic field descriptors were calculated using Lennard–Jones potential and Coulombic potential, respectively. For comparative similarity indices analysis (CoMSIA), the steric, electrostatic, hydrophobic and hydrogen bond donor and acceptors were calculated with Gaussian function, in contrast to distance-dependent dielectric method used in CoMFA. Partial least squares (PLS) regression was utilized to analyze the 3D-QSAR models, and all CoMFA and CoMSIA fields were taken as independent variables.

2.4. Molecular dynamics simulation

Selected TCM-mPGES-1 complexes were taken for molecular dynamics simulation. Each complex was solvated in a cubic water box before energetically minimized using 500 steps of Steepest Descent and 500 steps of Conjugate Gradient method. The system was then heated from 50 K to 310 K without constraint for 50 ps. The equilibration step was conducted for 200 ps without constraint. The final production step was conducted for 20 ns in NVT ensemble with snapshots save every 2.5 ps. The time step was set to 1 fs. Particle mesh Ewald (PME) was used for electrostatic calculation. Hydrogen bond frequency, energy trajectory, and hydrogen bond distance were calculated for analyzing the ligand–protein system.

3. Results and discussions

3.1. Docking and de novo design

The binding affinities of TCM ligands to the receptor were predicted based on scoring functions. We used Dock Score as the
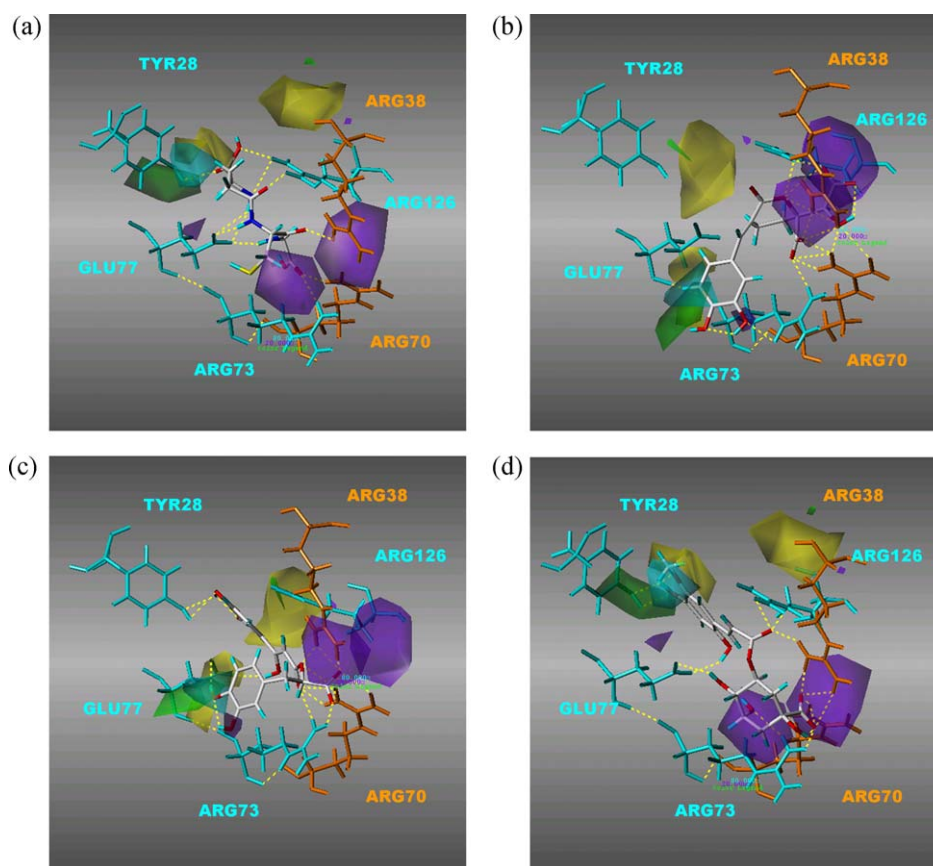
Fig. 3. The contour maps of CoMFA and CoMISA with (a) glutathione, (b) 2-O-caffeoyl tartaric acid-Evo_2, (c) glucogallin-Evo_1, and (d) 4-O-feruloylquinic acid-Evo_7 in the mPGES-1 binding site. Green and yellow contours indicate where steric groups would be favored or disfavored. Cyan and purple contours indicate where would be hydrophobic or hydrophilic. (For interpretation of the references to color in the figure caption, the reader is referred to the web version of the article.)
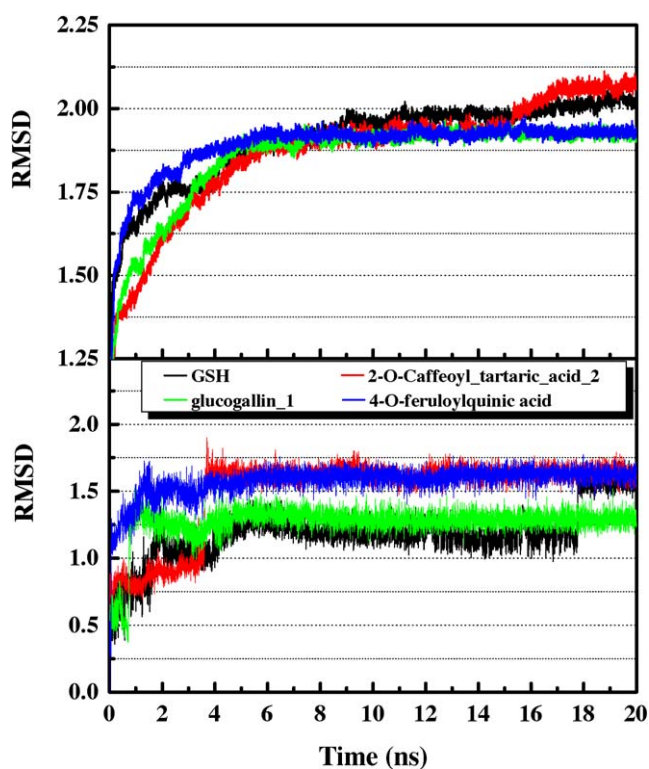
primary scoring function for ranking the ligands as this algorithm has been shown to correlate positively with actual bioactivity. TCM molecules ranked top in the docking are shown in Table 1; the top 10 compounds all have Dock Score higher than the control glutathione.

The top-ranking TCM derivatives, which all passed the ADMET screen, are shown in Table 2. As shown in Table 2, derivative of 2-O-caffeoyl tartaric acid derivative, 4-O-feruloylquinic acid derivative and glucogallin all have substantial increase in binding affinities as compared to the parental compounds. The structures of the top three derivatives and glutathione are shown in Table 3.
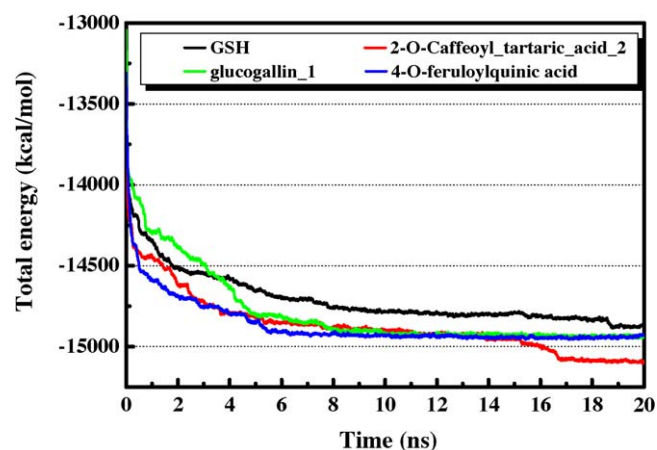

Fig. 4. The all atoms RMSD (top) and ligand RMSD (bottom) of mPGES-1–ligand complexes.

Fig. 5. The total energy for mPGES-1 complexes during 20 ns simulation.
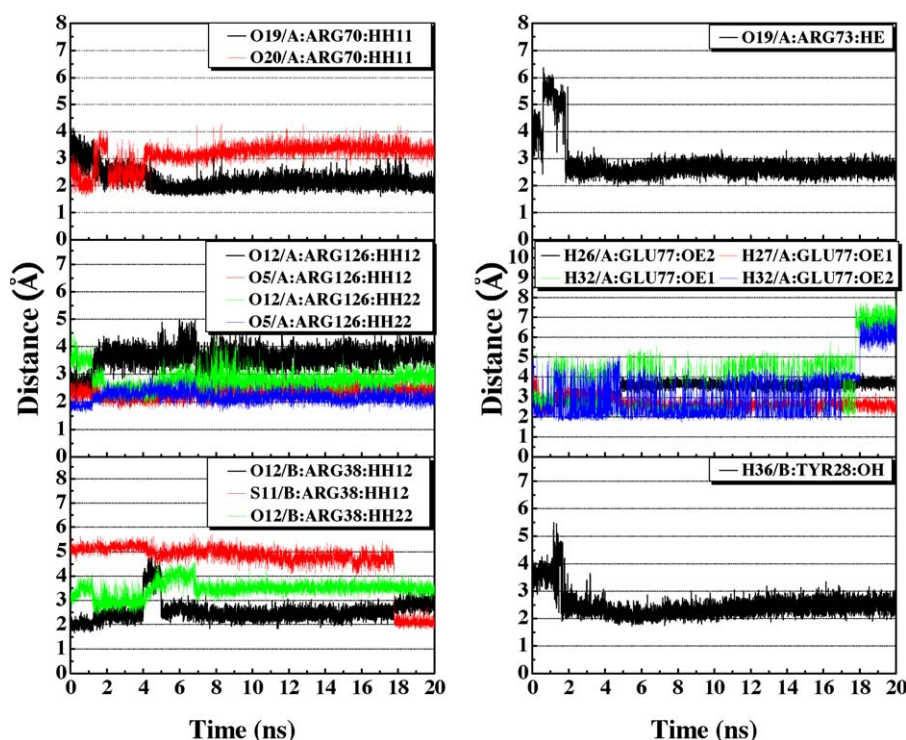
Fig. 6. Time dependent hydrogen bond distances between glutathione and mPGES-1 residues.

The docking conformations of these three derivatives are shown in Fig. 1. A conserved hydrogen bond network is formed between the mPGES-1 binding site residues and all the TCM molecules and the control. The key interacting residues are Arg38, Arg70, Arg73, Arg110 and Arg126 (Fig. 1).

3.2. CoMFA/CoMSIA

The structure and the experimental IC_{50} of the training set and the test set are shown in Table 4. The core atoms used in alignment are shown in Table 4 as well. The results for CoMFA and CoMSIA are

Table 7
Hydrogen bond statistics summary for glutathione.

| Ligand	Amino acid	Max. distance	Min. distance	Average distance	H-bond occupancy
O16	A:ARG110:HH11	3.81	2.01	3.04	5.33%
O16	A:ARG110:HH12	3.50	1.83	2.71	16.06%
O16	A:ARG110:HH22	4.20	2.27	3.09	0.48%
N7	A:ARG126:HH11	5.25	1.94	3.66	0.33%
N7	A:ARG126:HH12	4.86	2.24	3.13	0.38%
O12	A:ARG126:HH12	5.01	2.17	3.60	1.38%
O5	A:ARG126:HH12	3.15	1.70	2.33	76.91%
O12	A:ARG126:HH21	5.61	2.36	3.24	0.05%
O12	A:ARG126:HH22	4.53	1.84	2.78	19.60%
O5	A:ARG126:HH22	2.96	1.58	2.19	92.25%
O19	A:ARG70:HH11	4.14	1.60	2.21	83.70%
O20	A:ARG70:HH11	4.28	1.59	3.15	11.40%
O19	A:ARG73:HE	6.37	1.97	2.83	25.40%
O20	A:ASN74:HD22	5.15	2.39	3.60	0.04%
H37	A:ASN74:OD1	5.44	1.73	2.88	18.35%
H26	A:GLU77:OE2	4.19	2.18	3.44	0.99%
H27	A:GLU77:OE1	4.51	1.96	2.70	23.90%
H32	A:GLU77:OE1	7.98	1.90	3.57	38.46%
H32	A:GLU77:OE2	7.09	1.75	3.15	52.56%
H36	A:GLN134:OE1	5.93	2.44	4.09	0.01%
H27	A:HIS113:NE2	4.90	1.86	3.04	12.25%
H28	A:HIS113:NE2	4.41	2.00	3.29	3.61%
H36	A:TYR130:O	5.55	1.70	4.40	7.84%
O12	B:ARG38:HH12	4.78	1.67	2.55	56.71%
S11	B:ARG38:HH12	6.21	1.78	4.61	11.05%
O12	B:ARG38:HH22	4.61	2.33	3.47	0.23%
S11	B:CYS68:HG	8.71	2.46	6.47	0.01%
H32	B:CYS68:SG	8.47	1.95	6.35	0.81%
H26	B:HIS72:NE2	4.92	2.29	3.06	0.39%
H32	B:HIS72:NE2	5.90	1.88	3.57	4.80%
O16	B:TYR28:HH	5.40	2.31	4.47	0.05%
H36	B:TYR28:OH	5.50	1.73	2.48	61.39%
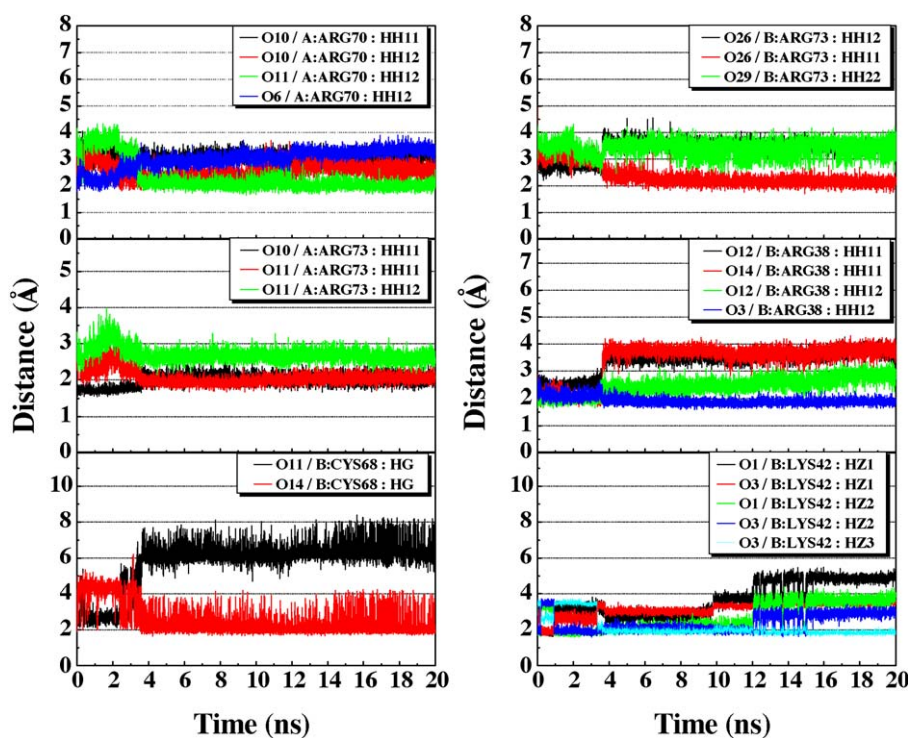
Fig. 7. Time dependent hydrogen bond distances between 2-O-caffeoyl tartaric acid-Evo_2 with mPGES-1 residues.
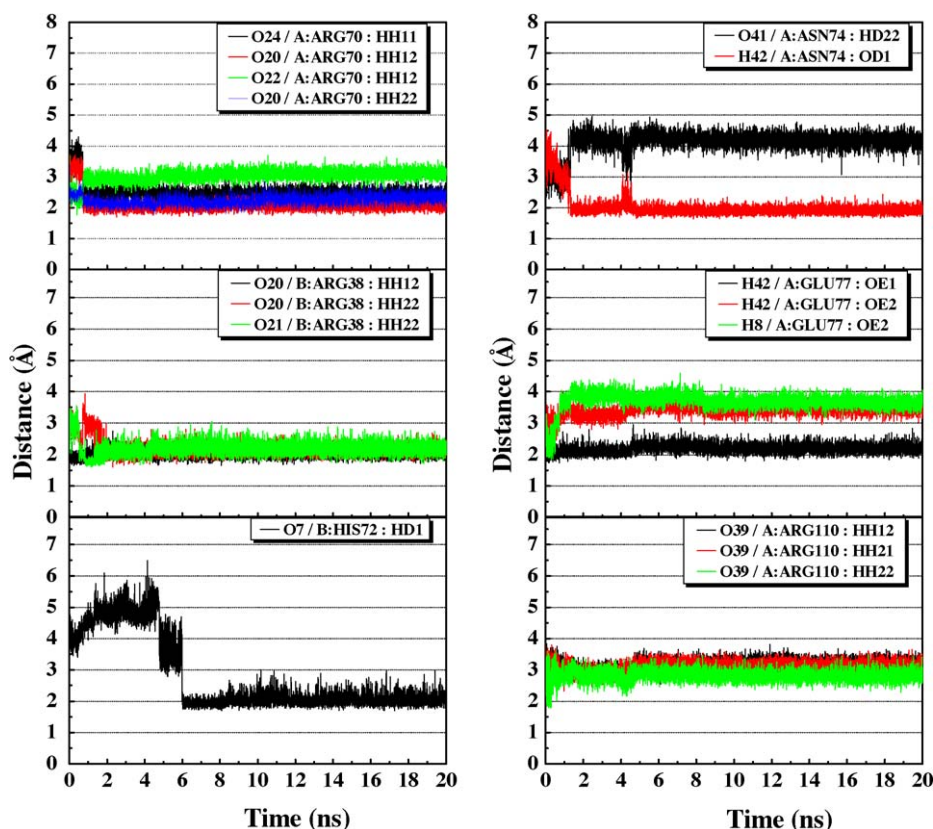
Fig. 8. Time dependent hydrogen bond distances between glucogallin-Evo_1 and mPGES-1 residues.

shown in Table 5. The CoMFA model has a non-cross-validated coefficient of 0.960 and a cross-validated coefficient of 0.597 (Fig. 2). As for the CoMSIA model, we selected the model containing steric, hydrophobic and hydrogen bond donor descriptor. For CoMSIA, the non-cross-validated coefficient is 0.931 and the cross-validation coefficient is 0.719 (Fig. 2). The activities predicted by CoMFA and CoMSIA, for both the training set and the test set, are shown in Table 6. Most predicted pIC_{50} only deviate less than one-fifth of log order from the experimental pIC_{50}. These values suggest that the CoMFA and CoMSIA models are reliable.

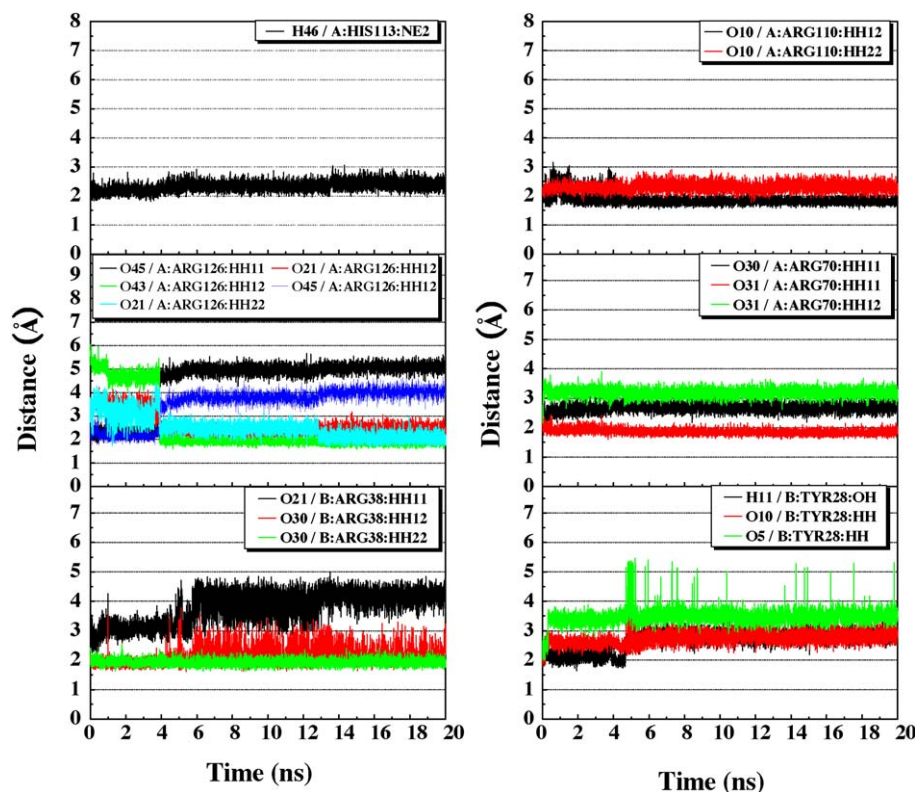**Fig. 9.** Time dependent hydrogen bond distances between 4-O-feruloylquinic acid-Evo_7 and mPGES-1 residues.

Table 8
Hydrogen bond statistics summary for 2-O-caffeoyl tartaric acid-Evo_2.

Ligand	Amino acid	Max. distance	Min. distance	Average distance	H-bond occupancy
H27	A:HIS72:O	6.338	1.617	2.72	24.04%
H7	A:TYR117:OH	3.994	1.83	3.48	0.15%
O1	A:ARG126:HE	3.964	1.818	2.99	11.39%
O10	A:ARG70:HH11	4.068	1.868	3.09	1.29%
O10	A:ARG70:HH12	3.836	1.808	2.59	39.41%
O11	A:ARG70:HH12	4.334	1.649	2.29	82.53%
O6	A:ARG70:HH12	3.907	1.78	3.9071	11.41%
O10	A:ARG73:HH11	2.558	1.543	1.97	99.96%
O11	A:ARG73:HH11	3.172	1.677	2.07	94.36%
O11	A:ARG73:HH12	3.978	2.138	2.70	11.70%
O6	A:TYR117:HH	4.136	1.765	2.73	12.43%
O12	B:ARG38:HH11	4.262	1.815	3.37	9.23%
O14	B:ARG38:HH11	4.321	1.692	3.43	17.70%
O1	B:ARG38:HH12	3.697	1.76	2.46	58.15%
O11	B:ARG38:HH12	5.923	1.821	4.70	4.74%
O12	B:ARG38:HH12	3.37	1.636	2.46	55.35%
O3	B:ARG38:HH12	2.879	1.588	1.92	99.71%
O3	B:ARG38:HH22	4.091	1.633	2.40	59.25%
O26	B:ARG73:HH12	4.551	2.215	3.40	5.61%
O11	B:CYS68:HG	8.382	2.119	5.75	2.65%
O14	B:CYS68:HG	6.206	1.651	2.52	72.66%
O1	B:LYS42:HZ1	5.493	1.633	3.69	6.36%
O3	B:LYS42:HZ1	3.87	1.654	3.15	6.91%
O1	B:LYS42:HZ2	4.392	1.591	2.68	57.26%
O3	B:LYS42:HZ2	3.737	1.6	2.39	56.01%
O1	B:LYS42:HZ3	3.915	2.139	3.18	0.20%
O3	B:LYS42:HZ3	3.81	1.552	2.13	83.90%
O1	A:ARG126:HH21	4.056	2.392	3.10	0.15%
O14	B:ARG38:HH12	4.263	2.441	3.49	0.03%
O26	B:ARG73:HH11	4.93	1.71	2.37	77.23%
O29	B:ARG73:HH22	4.31	2.453	3.44	0.05%
O11	A:ARG70:HH22	5.298	2.244	3.70	0.34%
H27	A:MET76:SD	5.739	2.136	2.92	13.66%
O11	A:ARG70:HH11	5.511	2.095	3.70	0.13%
O12	B:ARG38:HH22	4.715	2.391	3.38	0.08%

Table 9
Hydrogen bond statistics summary for Glucogallin-Evo_1.

Ligand	Amino acid	Max. distance	Min. distance	Average distance	H-bond occupancy
O39	A:ARG110:HH12	3.85	1.97	3.14	0.08%
O39	A:ARG110:HH21	3.89	2.32	3.13	0.01%
O39	A:ARG110:HH22	3.61	1.79	2.81	3.86%
O24	A:ARG70:HH11	4.31	1.79	2.46	66.54%
O20	A:ARG70:HH12	3.72	1.71	2.09	96.45%
O22	A:ARG70:HH12	3.73	1.78	3.04	2.48%
O24	A:ARG70:HH12	4.01	2.20	2.73	7.93%
O20	A:ARG70:HH22	4.34	1.74	2.25	91.29%
O22	A:ARG70:HH22	5.74	2.50	4.27	0.01%
O24	A:ARG73:HH11	3.99	2.29	2.79	1.13%
O41	A:ASN74:HD22	4.96	2.18	4.13	0.23%
O36	A:GLN134:HE22	5.32	2.01	4.05	2.98%
O20	A:TYR117:HH	5.48	2.24	3.40	1.59%
O20	B:ARG38:HH12	2.74	1.66	2.03	99.94%
O21	B:ARG38:HH12	3.52	1.96	2.59	34.83%
O22	B:ARG38:HH12	4.12	2.17	2.65	9.48%
O20	B:ARG38:HH22	3.94	1.61	2.20	91.53%
O21	B:ARG38:HH22	3.56	1.60	2.21	91.88%
H37	B:ALA31:O	4.17	2.05	3.49	1.00%
H40	A:GLU77:OE1	5.01	2.19	4.32	0.25%
H40	B:TYR28:OH	5.34	1.90	4.42	3.00%
H42	A:ASN74:OD1	4.53	1.63	2.02	93.35%
H42	A:GLU77:OE1	2.95	1.74	2.19	97.49%
H42	A:GLU77:OE2	4.00	2.41	3.42	0.08%
H8	A:GLU77:OE2	4.58	1.84	3.69	1.51%
O21	A:ARG70:HH22	4.37	2.18	3.08	1.10%
O21	B:CYS68:HG	5.74	2.00	4.06	1.94%
H37	B:TYR28:OH	5.64	2.48	4.53	0.01%
O7	B:HIS72:HD1	6.49	1.70	2.78	68.90%
H37	A:TYR130:O	5.93	2.28	3.45	0.69%

To compare our TCM derivatives with experimentally tested mPGES-1 inhibitors, we mapped the TCM derivatives into the CoMFA/CoMSIA contours. We only show the contour map from CoMSIA as it has covered the force field in CoMFA. As illustrated in Fig. 3, in addition to glutathione, all TCM derivatives map well into the CoMSIA contours. The hydrophilic contours are indicated by purple color, and the hydrophobic contours are shown in cyan. The green and yellow contours represent where adding steric group would be favored or disfavored. The top three TCM derivatives all contain hydrophilic groups and can form hydrogen bond interac-

tions to Arg70 and Arg38. These hydrogen bond interactions are all mapped onto the purple contours, which are in well agreement with the QSAR model. The contour maps can also be superimposed onto to corresponding residues of the mPGES-1 binding site. This further supports the docking result of the top TCM derivatives.

3.3. Molecular dynamics simulation

The top TCM derivatives and the control were selected for molecular dynamics simulation. The whole complex RMSD (top)

Table 10
Hydrogen bond statistics summary for 4-O-feruloylquinic acid-Evo_7.

Ligand	Amino acid	Max. distance	Min. distance	Average distance	H-bond occupancy
H11	B:TYR28:OH	3.68	1.64	2.67	24.65%
H40	A:GLU77:OE2	3.94	2.44	3.00	0.10%
H44	B:HIS72:NE2	6.27	2.07	5.57	0.28%
H46	A:HIS113:NE2	3.05	1.81	2.33	83.70%
O10	A:ARG110:HH12	3.16	1.53	1.86	97.19%
O10	A:ARG110:HH22	2.90	1.78	2.32	87.91%
O43	A:ARG126:HH11	6.92	2.18	3.15	7.41%
O45	A:ARG126:HH11	5.66	1.84	4.48	17.06%
O21	A:ARG126:HH12	4.21	1.84	2.61	59.19%
O43	A:ARG126:HH12	6.07	1.59	2.46	80.46%
O45	A:ARG126:HH12	4.67	1.73	3.54	18.75%
O45	A:ARG126:HH21	6.84	1.95	3.39	10.60%
O21	A:ARG126:HH22	4.43	1.65	2.49	58.54%
O45	A:ARG126:HH22	6.24	1.72	2.74	68.58%
O30	A:ARG70:HH11	3.47	2.09	2.69	10.54%
O31	A:ARG70:HH11	2.44	1.61	1.86	100.00%
O30	A:ARG70:HH12	3.49	2.18	2.90	1.55%
O31	A:ARG70:HH12	3.90	2.15	3.20	0.05%
O31	A:TYR117:HH	4.45	2.26	3.60	0.04%
O5	A:GLN134:HE21	4.20	2.25	3.06	0.04%
O21	B:ARG38:HH11	4.98	2.25	3.80	0.44%
O30	B:ARG38:HH12	3.78	1.61	2.09	92.28%
O30	B:ARG38:HH22	2.54	1.62	1.92	99.99%
O32	B:ARG38:HH22	3.98	1.91	3.34	0.25%
O10	B:TYR28:HH	4.20	1.79	2.75	10.73%
O5	B:TYR28:HH	5.47	2.00	3.48	1.00%

and the ligand RMSD (bottom) are shown in Fig. 4. All the ligand–protein complexes have reached equilibration during the simulation period. However, the glutathione–mPGES-1 complex has an increase in whole molecule and ligand RMSD value at 18 ns. In physiological state, binding of glutathione to mPGES-1 induces a conformational change in binding site residues, allowing for effective conversion of PGH_2 to PGE_2. We, therefore, attribute this increase ligand RMSD to changes in protein conformation. The energy trajectories of for all ligand–mPGES-1 complexes are shown in Fig. 5. All derivative–protein complexes have total energy lower than the control.

For the control, the most significant fluctuation in hydrogen bond distances appears in the beginning of the simulation run and at 18 ns (Fig. 6). The shift in interaction distance may be because the system is yet to adapt equilibration. At 18 ns, more hydrogen bonds are formed between the control and Arg38; on the contrary, interactions to Glu77 decrease (Table 7 and Supplementary video 1). As illustrated earlier, this is due to changes in both protein and ligand conformation.

For all the TCM derivatives, 2-O-caffeoyl tartaric acid-Evo_2, glucogallin-Evo_1 and 4-O-feruloylquinic acid-Evo_7, all have very stable interactions to binding site residues, with no obvious change in binding distances (Figs. 7–9). The carboxyl and carbonyl group of 2-O-caffeoyl tartaric acid-Evo_2 have H-bond interaction with residue Cys68 or Arg38 before the 4 ns of simulation (Supplementary video 2). Afterwards, at the following stable stage of simulation, the interaction was formed between 2-O-caffeoyl tartaric acid-Evo_2 and Arg38 shifts to between 2-O-caffeoyl tartaric acid-Evo_2 and Arg73 (Table 8 and Supplementary video 2). The interaction between glucogallin-Evo_1 hydroxyl group and Arg38 and Arg70 persist throughout the simulation time (Fig. 8 and Supplementary video 3). In addition, after equilibration hydrogen bond interactions are also found between glucogallin-Evo_1 and Asn74 and His7 (Table 9), which further strengthens the interaction between the derivative and binding site residues (Supplementary video 3). Similar to other TCM derivatives, 4-O-feruloylquinic acid-Evo_7 also established stable H-bonds with Arg38 and Arg70 as observed from hydrogen bond statistics (Table 10), hydrogen bond distance (Fig. 9) and Supplementary video 4. Overall, the TCM derivatives all have stable and continuous hydrogen bond interaction to binding site residues; these interactions keep the derivative firmly bonded to mPGES-1 glutathione binding site.

4. Conclusion

To identify new anti-inflammatory molecules, docking of TCM molecules into mPGES-1 glutathione bind site was performed. Subsequent *de novo* design generated 2-O-caffeoyl tartaric acid_2, glucogallin_1 and 4-O-feruloylquinic acid_7 that serve great potential as next generation of anti-inflammatory compounds. These derivatives were selected for further analyses using QSAR and molecular dynamics simulation. Both the CoMFA and CoMSIA models investigated had high non-cross-validation coefficient of r^2 of 0.960 and 0.719 and high cross-validation coefficient q^2 of 0.597 and 0.719. The top three derivatives were able to map onto the steric, hydrophobic and hydrogen bond donor fields of CoMSIA, meeting the requirements of being effective mPGES-1 inhibitor. Analyses of molecular dynamics simulation showed that the TCM derivatives have continuous and stable hydrogen bond interactions to key binding site residues, Arg38 and Arg70. In addition, extensive hydrogen bond networks were formed between the TCM derivatives and the mPGES-1 binding site residues. This event suggests that the top three TCM derivatives can bind strongly to mPGES-1 residues, making them very potent candidates.

Appendix A. Supplementary data

Supplementary data associated with this article can be found, in the online version, at doi:10.1016/j.jtice.2010.11.009.

References

Bohm, H. J., "The Computer Program Ludi: A New Method for the *De Novo* Design of Enzyme Inhibitors," *J. Comput. Aided Mol. Des.*, **6**, 61 (1992).

Bohm, H. J., "Prediction of Binding Constants of Protein Ligands: A Fast Method for the Prioritization of Hits Obtained from *De Novo* Design or 3d Database Search Programs," *J. Comput. Aided Mol. Des.*, **12**, 309 (1998).

Chang, T. T., H. J. Huang, K. J. Lee, H. W. Yu, H. Y. Chen, F. J. Tsai, M. F. Sun, and C. Y. C. Chen, "Key Features for Designing Phosphodiesterase-5 Inhibitors," *J. Biomol. Struct. Dyn.*, **28**, 309 (2010).

Chen, C. Y. C., "Discovery of Novel Inhibitors for C-Met by Virtual Screening and Pharmacophore Analysis," *J. Chin. Inst. Chem. Engrs.*, **39**, 617 (2008).

Chen, C. Y. C., "Chemoinformatics and Pharmacoinformatics Approach for Exploring the Gaba-a Agonist from Chinese Herb Suanzaoren," *J. Taiwan Inst. Chem. Engrs.*, **40**, 36 (2009a).

Chen, C. Y. C., "Computational Screening and Design of Traditional Chinese Medicine (Tcm) to Block Phosphodiesterase-5," *J. Mol. Graph. Model.*, **28**, 261 (2009b).

Chen, C. Y. C., "De Novo Design of Novel Selective Cox-2 Inhibitors: From Virtual Screening to Pharmacophore Analysis," *J. Taiwan Inst. Chem. Engrs.*, **40**, 55 (2009c).

Chen, C. Y. C., "Magnolol Encapsulated by Different Acyl Chain Length of Liposomes on Inhibiting Proliferation of Smooth Muscle Cells," *J. Taiwan Inst. Chem. Engrs.*, **40**, 380 (2009d).

Chen, C. Y. C., "Pharmacoinformatics Approach for Mpges-1 in Anti-Inflammation by 3d-Qsar Pharmacophore Mapping," *J. Taiwan Inst. Chem. Engrs.*, **40**, 155 (2009e).

Chen, C. Y. C., "Weighted Equation and Rules—A Novel Concept for Evaluating Protein–Ligand Interaction," *J. Biomol. Struct. Dyn.*, **27**, 271 (2009f).

Chen, C. Y. C., "Bioinformatics, Chemoinformatics, and Pharmainformatics Analysis of Her2/Hsp90 Dual-Targeted Inhibitors," *J. Taiwan Inst. Chem. Engrs.*, **41**, 143 (2010a).

Chen, C. Y. C., "Virtual Screening and Drug Design for Pde-5 Receptor from Traditional Chinese Medicine Database," *J. Biomol. Struct. Dyn.*, **27**, 627 (2010b).

Chen, C. Y., Y. H. Chang, D. T. Bau, H. J. Huang, F. J. Tsai, C. H. Tsai, and C. Y. C. Chen, "Discovery of Potent Inhibitors for Phosphodiesterase 5 by Virtual Screening and Pharmacophore Analysis," *Acta Pharmacol. Sin.*, **30**, 1186 (2009a).

Chen, C. Y., Y. H. Chang, D. T. Bau, H. J. Huang, F. J. Tsai, C. H. Tsai, and C. Y. C. Chen, "Ligand-based Dual Target Drug Design for H1N1: Swine Flu-a Preliminary First Study," *J. Biomol. Struct. Dyn.*, **27**, 171 (2009b).

Chen, Y. C. and K. T. Chen, "Novel Selective Inhibitors of Hydroxyxanthone Derivatives for Human Cyclooxygenase-2," *Acta Pharmacol. Sin.*, **28**, 2027 (2007).

Chen, C. Y. and C. Y. C. Chen, "Insights into Designing the Dual-Targeted Her2/Hsp90 Inhibitors," *J. Mol. Graph. Model.*, **29**, 21 (2010a).

Chen, C. Y., H. J. Huang, F. J. Tsai, and C. Y. C. Chen, "Drug Design for Influenza a Virus Subtype H1N1," *J. Taiwan Inst. Chem. Engrs.*, **41**, 8 (2010a).

Chen, C. Y., P. L. Kuo, Y. H. Chen, J. C. Huang, M. L. Ho, R. J. Lin, J. S. Chang, and H. M. Wang, "Tyrosinase Inhibition, Free Radical Scavenging, Antimicroorganism and Anticancer Proliferation Activities of Sapindus Mukorossi Extracts," *J. Taiwan Inst. Chem. Engrs.*, **41**, 129 (2010b).

Giroux, A., L. Boulet, C. Brideau, A. Chau, D. Claveau, B. Cote, D. Ethier, R. Frenette, M. Gagnon, J. Guay, S. Guiral, J. Mancini, E. Martins, F. Masse, N. Methot, D. Riendeau, J. Rubin, D. Xu, H. Yu, Y. Ducharme, and R. W. Friesen, "Discovery of Disubstituted Phenanthrene Imidazoles as Potent, Selective and Orally Active Mpges-1 Inhibitors," *Bioorg. Med. Chem. Lett.*, **19**, 5837 (2009).

Hara, S., D. Kamei, Y. Sasaki, A. Tanemoto, Y. Nakatani, and M. Murakami, "Prostaglandin E Synthases: Understanding Their Pathophysiological Roles through Mouse Genetic Models," *Biochimie*, **92**, 651 (2010).

Huang, H. J., C. Y. Chen, H. Y. Chen, F. J. Tsai, and C. Y. C. Chen, "Computational Screening and Qsar Analysis for Design of Amp-Activated Protein Kinase Agonist," *J. Taiwan Inst. Chem. Engrs.*, **41**, 352 (2010a).

Huang, H. J., K. J. Lee, H. W. Yu, C. Y. Chen, C. H. Hsu, H. Y. Chen, F. J. Tsai, and C. Y. C. Chen, "Structure-based and Ligand-based Drug Design for Her 2 Receptor," *J. Biomol. Struct. Dyn.*, **28**, 23 (2010b).

Huang, H. J., K. J. Lee, H. W. Yu, H. Y. Chen, F. J. Tsai, and C. Y. C. Chen, "A Novel Strategy for Designing the Selective Ppar Agonist by The Sum of Activity Model," *J. Biomol. Struct. Dyn.*, **28**, 187 (2010c).

Jain, A. N., "Scoring Noncovalent Protein–Ligand Interactions: A Continuous Differentiable Function Tuned to Compute Binding Affinities," *J. Comput. Aided Mol. Des.*, **10**, 427 (1996).

Jegerschold, C., S. C. Pawelzik, P. Purhonen, P. Bhakat, K. R. Gheorghe, N. Gyobu, K. Mitsuoka, R. Morgenstern, P. J. Jakobsson, and H. Hebert, "Structural Basis for Induced Formation of the Inflammatory Mediator Prostaglandin E2," *Proc. Natl. Acad. Sci. U.S.A.*, **105**, 11110 (2008).

Koeberle, A. and O. Werz, "Inhibitors of the Microsomal Prostaglandin E-2 Synthase-1 as Alternative to Non Steroidal Anti-Inflammatory Drugs (Nsaids)—A Critical Review," *Curr. Med. Chem.*, **16**, 4274 (2009).

Lin, M. L., Y. C. Lu, J. G. Chung, S. G. Wang, H. T. Lin, S. E. Kang, C. H. Tang, J. L. Ko, and S. S. Chen, "Down-Regulation of Mmp-2 through the P38 Mapk-Nf-Kappa B-Dependent Pathway by Aloe-Emodin Leads to Inhibition of Nasopharyngeal Carcinoma Cell Invasion," *Mol. Carcinog.*, **49**, 783 (2010).

Lipinski, C. A., F. Lombardo, B. W. Dominy, and P. J. Feeney, "Experimental and Computational Approaches to Estimate Solubility and Permeability in Drug Discovery and Development Settings," *Adv. Drug Deliv. Rev.*, **46**, 3 (2001).

Liu, J. F., W. H. Yang, Y. C. Fong, S. C. Kuo, C. S. Chang, and C. H. Tang, "Bfpp, a Phloroglucinol Derivative. Induces Cell Apoptosis in Human Chondrosarcoma Cells through Endoplasmic Reticulum Stress," *Biochem. Pharmacol.*, **79**, 1410 (2010).

Lo, C., T. Y. Lai, J. H. Yang, J. S. Yang, Y. S. Ma, S. W. Weng, Y. Y. Chen, J. G. Lin, and J. G. Chung, "Gallic Acid Induces Apoptosis in A375.S2 Human Melanoma Cells through Caspase-Dependent and -Independent Pathways," *Int. J. Oncol.*, **37**, 377 (2010).

Mancini, J. A., K. Blood, J. Guay, R. Gordon, D. Claveau, C. C. Chan, and D. Riendeau, "Cloning, Expression, and up-Regulation of Inducible Rat Prostaglandin E Synthase during Lipopolysaccharide-induced Pyresis and Adjuvant-induced Arthritis," *J. Biol. Chem.*, **276**, 4469 (2001).

Muegge, I. and Y. C. Martin, "A General and Fast Scoring Function for Protein–Ligand Interactions: A Simplified Potential Approach," *J. Med. Chem.*, **42**, 791 (1999).

Venkatachalam, C. M., X. Jiang, T. Oldfield, and M. Waldman, "Ligandfit: A Novel Method for the Shape-Directed Rapid Docking of Ligands to Protein Active Sites," *J. Mol. Graph. Model.*, **21**, 289 (2003).